Title	ナローギャップ・ワイドギャップIII-V族化合物半導体デバイスにおける低周波雑音
Author(s)	Le, Phuong Son
Citation	
Issue Date	2014-09
Type	Thesis or Dissertation
Text version	ETD
URL	http://hdl.handle.net/10119/12304
Rights	
Description	Supervisor:鈴木　寿一，マテリアルサイエンス研究科，博士

Low-frequency noise in narrow- and wide-gap III-V compound semiconductor devices

Suzuki Laboratory s1140211 LE Phuong Son

1 Introduction

III-V compound semiconductors, which have many advantages over silicon, are important materials for electronic and optical devices. For example, InAs, which has a narrow energy gap E_g and a very high electron mobility μ, is a potential material for high-speed device applications. In contrast to InAs, GaN, which has a wide E_g and a moderate μ, is a promising material for high-power device applications. Although III-V compound semiconductor devices have been studied for a long time [1–3], their low-frequency noise (LFN) characterization still remains many issues.

In this work, we fabricated two-terminal (2T) devices from InAs films obtained by separation-bonding method on low-k flexible substrates (FS) (InAs/FS) [4, 5] or by direct growth on GaAs(001) (InAs/GaAs). In addition, from $\mathrm{Al}_{0.27}\mathrm{Ga}_{0.73}\mathrm{N}/\mathrm{GaN}$ heterostructures, we fabricated GaN devices, ungated 2T devices as well as heterojunction field-effect transistors (HFETs), with Schottky structures and metal-insulator-semiconductor (MIS) structures in which an AlN insulator was sputtering-deposited on the AlGaN [6, 7]. Before the AlN deposition, two types of the AlGaN surface treatment were used with and without a cleaning by Semicoclean (an ammonium-based solution, ABS). Using these devices, LFN in InAs and GaN devices were investigated by using a measurement system with configurations shown in Fig. 1(a) for 2T devices and (b) for HFETs.

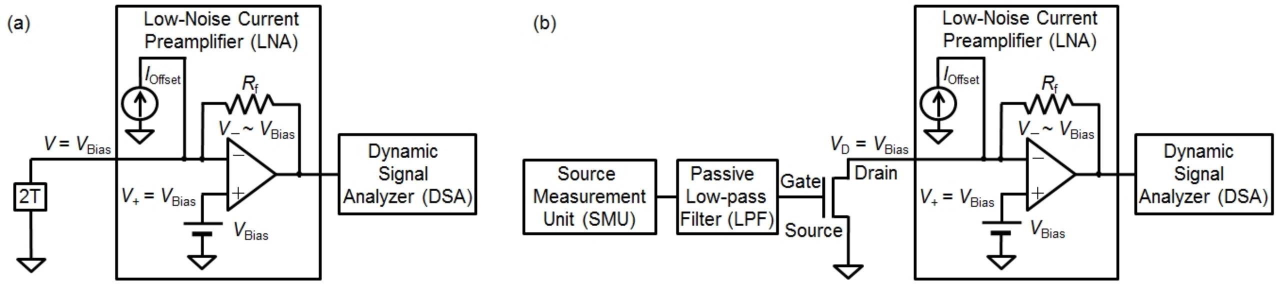

Figure 1: Low-frequency noise measurement system for (a) 2T devices and (b) HFETs.

2 Low-frequency noise in InAs films bonded on low-k flexible substrates or grown on GaAs(001)

Figures 2(a) and (b) show the mobility μ as functions of the InAs thickness d and the sheet electron concentration n_s, respectively. The LFN in InAs devices shown in Figs. 2(c) and (d) exhibits that the current noise power spectrum density S_I satisfies $S_I/I^2 \simeq K/f$ with current I and frequency f, where K is a constant.

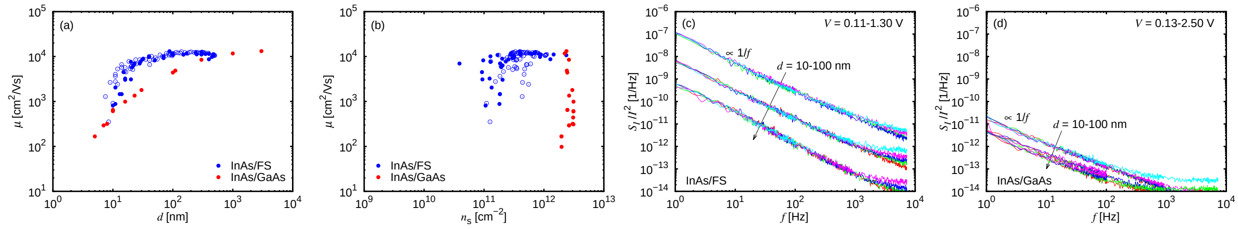

Figure 2: The mobility μ as functions of (a) the InAs thickness d and (b) the sheet electron concentration n_s. S_I/I^2 as functions of f for (c) InAs/FS and (d) InAs/GaAs with $d \simeq 10,\ 30,\ 100$ nm.

Figures 3(a) and (b) show $S_I f$ as functions of I to determine K. Since the device resistance is the sum of the contact resistance $R_\mathrm{c} = r_\mathrm{c}/W$ and the InAs channel resistance $R_\mathrm{ch} = r_\mathrm{s}L/W$ with the contact resistivity r_c, the sheet resistance r_s, the channel length L, and the device width W, the factor K is given by

$$KW = \frac{(K_\mathrm{c}W/2) + (\alpha/n_\mathrm{s})(r_\mathrm{s}/2r_\mathrm{c})^2 L}{[1 + (r_\mathrm{s}/2r_\mathrm{c})L]^2}, \tag{1}$$

where K_c is the factor for one contact, α and n_s are the Hooge parameter and the sheet electron concentration of the InAs channel, respectively. Figures 3(c) and (d) show KW as functions of L with fitting lines using Eq. (1), exhibiting $K \propto 1/LW$, which indicates a negligible contribution of the contacts. The LFN is hence dominated by the channel, and the Hooge parameter can be calculated by $\alpha = KN = Kn_\mathrm{s}LW$, where N is the electron number in the InAs channel.

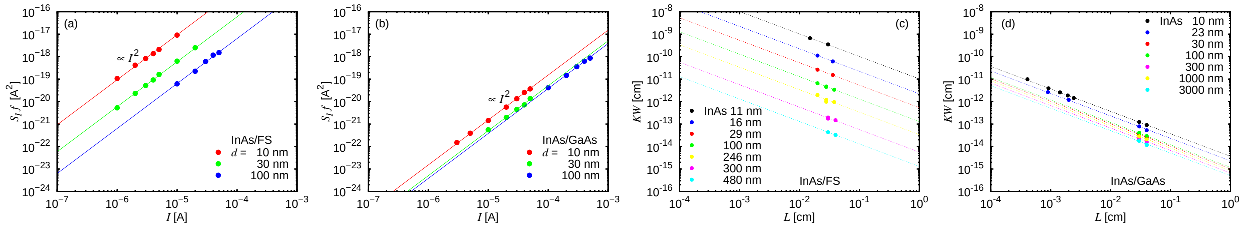

Figure 3: $S_I f$ as functions of I for (a) InAs/FS and (b) InAs/GaAs. The factor KW as functions of L for (c) InAs/FS and (d) InAs/GaAs.

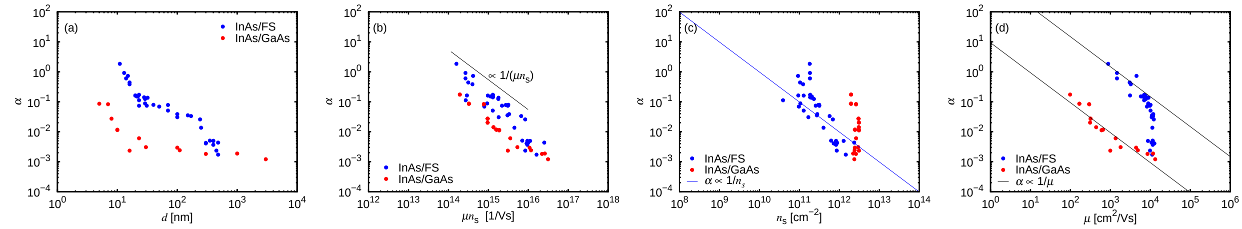

Figure 4: Hooge parameter α in InAs films as functions of (a) the InAs thickness d, (b) the product μn_s, (c) the sheet electron concentration n_s, and (d) the electron mobility μ.

Figure 4 shows α as functions of (a) d, (b) μn_s, (c) n_s, and (d) μ. The Hooge parameter is given by $\alpha = \dfrac{1}{\ln(f_\mathrm{h}/f_\ell)}\left(\dfrac{(\delta\mu)^2}{\mu^2} + \dfrac{(\delta N)^2}{N}\right)$, where f_h and f_ℓ are the high and low limits of the $1/f$ behavior [8]. For InAs/FS with $d \gtrsim 20$ nm, where μ weakly changes as seen in Fig. 2(b), $\alpha \propto {n_\mathrm{s}}^{-1}$ is observed and attributed to the carrier-number fluctuation $(\delta N)^2 \sim LWD_\mathrm{i}k_\mathrm{B}T$, where the interface state density $D_\mathrm{i} \sim 10^{12}$ cm^{-2}eV^{-1} is obtained from the data, being consistent with the Coulomb-scattering mobility [5]. For InAs/FS with $d \lesssim 20$ nm and InAs/GaAs(001), where n_s weakly changes as seen in Fig. 2(b), $\alpha \propto \mu^{-1}$ is observed, which can be related to the mobility fluctuation due to constant fluctuations in the InAs thickness.

3 Low-frequency noise in AlGaN/GaN heterostructure

Figure 5(a) shows the product of the resistance R and the device width W as functions of the electrode spacing L for ungated 2T GaN devices, exhibiting a significant contribution of the contacts. The LFN spectra shown in Figs. 5(b)-(d) exhibit that S_I satisfies $S_I/I^2 \simeq K/f$, where K is a constant depending on device size.

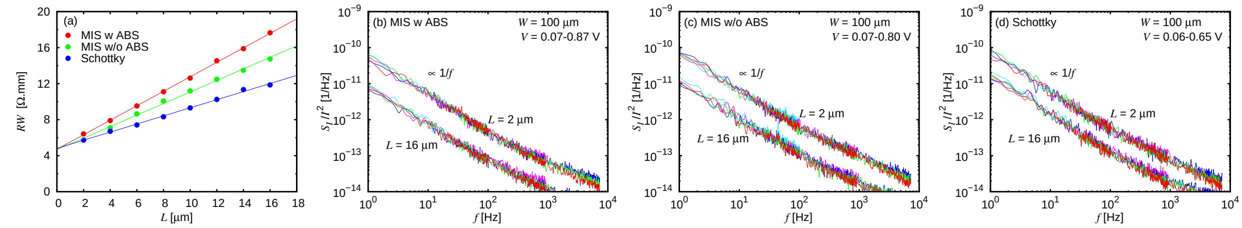

Figure 5: (a) The product of the resistance R and the device width W as functions of the electrode spacing L. S_I/I^2 as functions of f for GaN ungated 2T devices, (b) MIS w ABS, (c) MIS w/o ABS, and (d) Schottky devices.

Figures 6(a)-(c) show $S_I f$ as functions of I to determine K shown in Fig. 6(d). The ungated 2T GaN devices show $K \simeq$ constant for small L, indicating a significant contribution of the electrode contacts. Since the device resistance is the sum of the contact resistance and the ungated-channel resistance, we also obtained Eq. (1). Fitting data by Eq. (1), we obtained $K_\mathrm{c}W \simeq 1.9 \times 10^{-12}$ cm for one contact, which is common for the MIS and Schottky devices because of the same Ohmic process, and a Hooge parameter of the ungated region

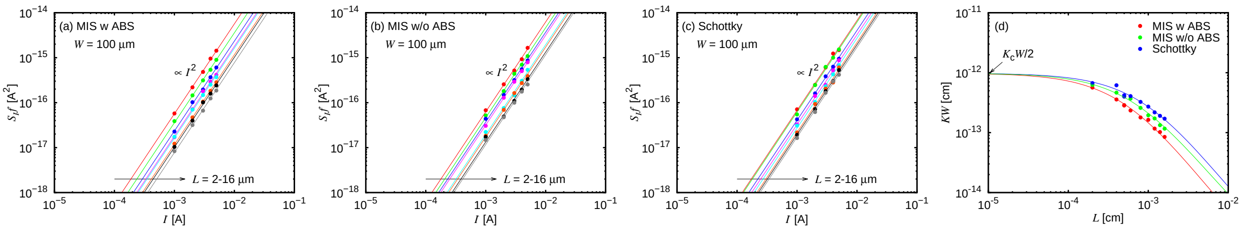

Figure 6: $S_I f$ as functions of I for GaN ungated 2T devices, (a) MIS w ABS, (b) MIS w/o ABS, and (c) Schottky devices. (d) The factor KW as functions of L for GaN ungated 2T devices.

$\alpha_{\rm ug} \simeq 2.2 \times 10^{-4}$ for the ungated 2T MIS devices with cleaning by ABS (w ABS), 4.1×10^{-4} for MIS devices w/o ABS, and 5.0×10^{-4} for Schottky devices. The smaller $\alpha_{\rm ug}$ in the MIS devices can be attributed to the lower electron mobility due to additional scattering mechanisms caused by the AlN insulator deposition, where the mobility fluctuation dominates $\alpha_{\rm ug}$ according to the Hooge theory [8].

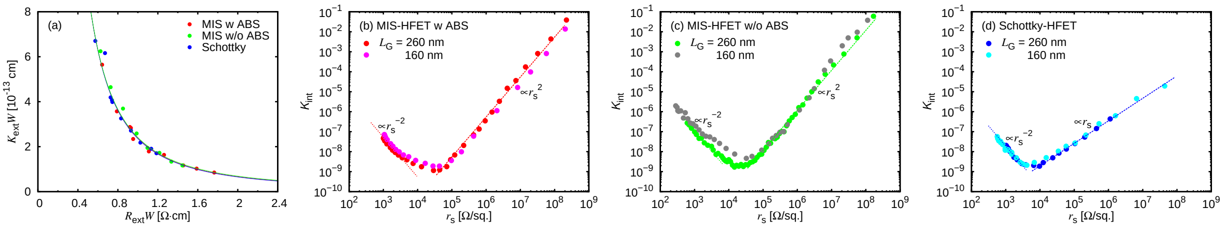

Figure 7: (a) $K_{\rm ext}W$ as functions of $R_{\rm ext}W$ for the ungated part of the GaN devices. The factor $K_{\rm int}$ as functions of the sheet resistance $r_{\rm s}$ of the gated region of GaN HFETs for (b) MIS w ABS, (c) MIS w/o ABS, and (d) Schottky devices.

The channel-current-dominated LFN in the linear regime of the GaN HFETs shows $S_{I_{\rm D}} \simeq K_{\rm HFET} {I_{\rm D}}^2/f$ with the drain current $I_{\rm D}$ and a constant factor $K_{\rm HFET}$ depending on the gate-source voltage $V_{\rm G}$. From the ungated-device characterization, LFN behavior in the intrinsic gated region was extracted for the HFETs. Since the on-resistance $R_{\rm on}$ given by the series connection of the intrinsic resistance $R_{\rm int} = r_{\rm s}L_{\rm G}/W$ with the sheet resistance $r_{\rm s}$ of the gated region and the gate length $L_{\rm G}$, and the extrinsic resistance $R_{\rm ext}$ of the ungated part,

$$K_{\rm HFET} = K_{\rm int}\frac{{R_{\rm int}}^2}{{R_{\rm on}}^2} + K_{\rm ext}\frac{{R_{\rm ext}}^2}{{R_{\rm on}}^2}, \tag{2}$$

where $K_{\rm int}$ is the factor for the intrinsic noise depending on $V_{\rm G}$, and $K_{\rm ext}$ is the factor for the extrinsic noise independent of $V_{\rm G}$. From the value of the $R_{\rm ext}$ obtained by DC characterization, we can evaluate $K_{\rm ext}$ of the ungated part using the relation given in Fig. 7(a), and consequently $K_{\rm int}$ by Eq. (2), as shown in Figs. 7(b)-(d). For the small $r_{\rm s}$ below the middle of 10^3 Ω/sq. range, $K_{\rm int} \propto {r_{\rm s}}^{-2}$ for both the MIS- and Schottky-HFETs. On the other hand, the MIS-HFETs for $r_{\rm s} \gtrsim 10^5$ Ω/sq. exhibit $K_{\rm int} \propto {r_{\rm s}}^2$, while the Schottky-HFETs for $r_{\rm s} \gtrsim 10^4$ Ω/sq. exhibit $K_{\rm int} \propto r_{\rm s}$. The factor $K_{\rm int}$ is given by $K_{\rm int} = \alpha/N = \alpha/n_{\rm s}L_{\rm G}W$, where $n_{\rm s}$ is the sheet electron concentration of the gated region. We obtained $n_{\rm s}$ by integration of the capacitance by measuring capacitors fabricated simultaneously with the HFETs. As a result, we obtain the Hooge parameter α as functions of $n_{\rm s}$, shown in Fig. 8 with the point of $\alpha_{\rm ug}$ for the ungated region.

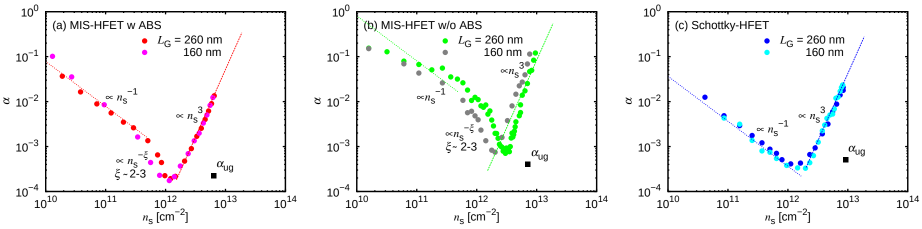

Figure 8: The Hooge parameter α as functions of the sheet electron concentration $n_{\rm s}$ of the gated region of GaN HFETs for (a) MIS w ABS, (b) MIS w/o ABS, and (c) Schottky devices. The point of $\alpha_{\rm ug}$ is for the ungated region.

For the MIS-HFETs with the small $n_{\rm s} \lesssim 5 \times 10^{11}$ cm^{-2}, $\alpha \propto {n_{\rm s}}^{-1}$, also observed for Schottky-HFETs with $n_{\rm s} \lesssim 10^{12}$ cm^{-2}, and is attributed to the carrier-number fluctuation due to electron traps with density

$D_0 \sim 10^{11}$ cm^{-2}eV^{-1} in the AlGaN. On the other hand, for 5×10^{11} cm$^{-2} \lesssim n_\mathrm{s} \lesssim 1 \times 10^{12}$ cm^{-2}, the MIS-HFETs show $\alpha \propto {n_\mathrm{s}}^{-\xi}$ with $\xi \sim$ 2-3, which is not observed for Schottky-HFETs, and tentatively attributed to the mobility fluctuation specific for the MIS-HFETs. Moreover, $\alpha \propto {n_\mathrm{s}}^3$ for both MIS- and Schottky-HFETs with $n_\mathrm{s} \gtrsim 2 \times 10^{12}$ cm^{-2}, can be attributed to the fluctuation in the intrinsic gate voltage, which is enhanced for large gate voltage and n_s by the fluctuation of the voltage across the extrinsic source resistance.

4 Conclusion

LFN in narrow- and wide-gap III-V compound semiconductors were systematically investigated for InAs (narrow-gap) and GaN (wide-gap) devices. We clarified detailed behaviors of the Hooge parameter depending on the devices.

References

[1] M. Tacano, M. Ando, I. Shibasaki, S. Hashiguchi, J. Sikula, and T. Matsui, Microelectron. Reliab. **40**, 1921 (2000).

[2] M. E. Levinshtein, F. Pascal, S. Contreras, W. Knap, S. L. Rumyantsev, R. Gaska, J. W. Yang, and M. Shur, Appl. Phys. Lett. **72**, 3053 (1998).

[3] N. Pala, R. Gaska, S. Rumyantsev, M. Shur, M. A. Khan, X. Hu, G. Simin, and J. Yang, Electron. Lett. **36**, 268 (2000).

[4] H. Takita, N. Hashimoto, C. T. Nguyen, M. Kudo, M. Akabori, and T. Suzuki, Appl. Phys. Lett. **97**, 012102 (2010).

[5] C. T. Nguyen, H.-A. Shih, M. Akabori, and T. Suzuki, Appl. Phys. Lett. **100**, 012102 (2012).

[6] H.-A. Shih, M. Kudo, M. Akabori, and T. Suzuki, Jpn. J. Appl. Phys. **51**, 02BF01 (2012).

[7] H.-A. Shih, M. Kudo, and T. Suzuki, Appl. Phys. Lett. **101**, 043501 (2012).

[8] F. N. Hooge, T. G. M. Kleinpenning, and L. K. J. Vandamme, Rep. Prog. Phys. **44**, 479 (1981).

Table of contents

List of publications

1. S. P. Le, M. Akabori and T. Suzuki: "Electron mobility anisotropy in InAs/GaAs(001)", The seventeenth International Conference on Molecular Beam Epitaxy, Nara, Japan, September 23-28 (2012).
2. S. P. Le, T. Q. Nguyen, H.-A. Shih, M. Kudo and T. Suzuki: "Low-frequency noise of intrinsic gated region in AlN/AlGaN/GaN metal-insulator-semiconductor heterojunction field-effect transistors", International Conference on Solid State Devices and Materials, Tsukuba, Japan, September 8-11 (2014).
3. S. P. Le, T. Q. Nguyen, H.-A. Shih, M. Kudo and T. Suzuki: "Low-frequency noise in AlN/AlGaN/GaN metal-insulator-semiconductor devices: a comparison with Schottky devices", Journal of Applied Physics **116** (2014) 054510.

Keywords

III-V compound semiconductors, InAs, AlGaN/GaN, low-frequency noise, Hooge parameter.